HHS Public Access

Author manuscript

Acta Biomater. Author manuscript; available in PMC 2022 December 01.

Published in final edited form as:

Acta Biomater. 2021 December ; 136: 88–98. doi:10.1016/j.actbio.2021.09.032.

Reversible dynamic mechanics of hydrogels for regulation of cellular behavior

Oju Jeon[1,2,*], **Tae-Hee Kim**[3], **Eben Alsberg**[1,2,4,5,*]

[1]Department of Biomedical Engineering, Case Western Reserve University, Cleveland, Ohio, 44106, USA

[2]Department of Biomedical Engineering, University of Illinois at Chicago, Chicago, Illinois, 60607, USA.

[3]Department of Medical Anthropology, Case Western Reserve University, Cleveland, Ohio, 44106, USA

[4]Department of Orthopaedic Surgery, Case Western Reserve University, Cleveland, Ohio, 44106, USA

[5]Departments of Orthopaedics, Pharmacology, and Mechanical & Industrial Engineering, University of Illinois at Chicago, Chicago, Illinois, 60607, USA

Abstract

The mechanical properties of the native extracellular matrix play a key role in regulating cell behavior during developmental, healing and homeostatic processes. Since these properties change over time, it may be valuable to have the capacity to dynamically vary the mechanical properties of engineered hydrogels used in tissue engineering strategies to better mimic the dynamic mechanical behavior of native extracellular matrix. However, *in situ* repeatedly reversible dynamic tuning of hydrogel mechanics is still limited. In this study, we have engineered a hydrogel system with reversible dynamic mechanics using a dual-crosslinkable alginate hydrogel. The effect of reversible mechanical signals on encapsulated stem cells in dynamically tunable hydrogels has been demonstrated. *In situ* stiffening of hydrogels decreases cell spreading and proliferation, and subsequent softening of hydrogels gives way to an increase in cell spreading and proliferation. The hydrogel stiffening and softening, and resulting cellular responses are repeatedly reversible. This hydrogel system provides a promising platform for investigating the effect of repeatedly reversible changes in extracellular matrix mechanics on cell behaviors.

[*]Corresponding authors. ojeon2@uic.edu (O. Jeon), ealsberg@uic.edu (E. Alsberg).

Author contributions

O.J. and E.A. conceived the ideas and designed the experiments. O.J. and T.K. conducted the experiments. O.J., T.K., and E.A. analyzed and interpreted the data and wrote the manuscript.

Declaration of interests

The authors declare that they have no known competing financial interests or personal relationships that could have appeared to influence the work reported in this paper.

Graphical Abstract

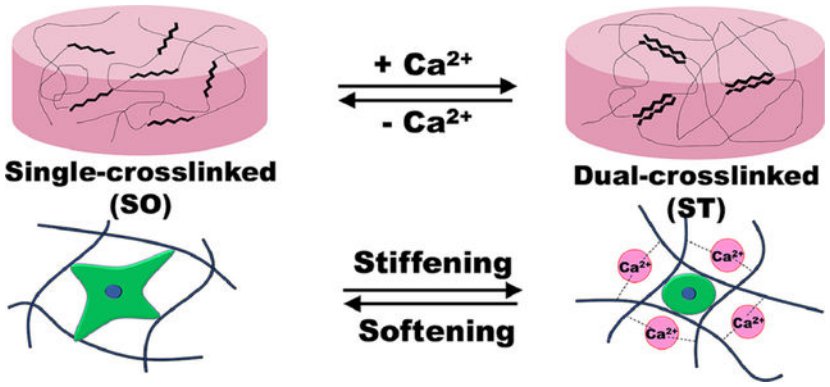

Keywords

dynamic mechanics; hydrogel; dual-crosslinking; stem cell

1. Introduction

Cells are continuously affected by biochemical and physical signals within their microenvironments that are continuously changing during biological processes including development, tissue regeneration and wound healing.[1, 2] Mimicking these cellular microenvironments by engineering biomaterial systems capable of controlled presentation of these signals in time and space may allow for investigation and better understanding of the effects of these cues on cell behavior.[3–7] With respect to biomaterial mechanical signals, it has been demonstrated that manipulating them can promote changes in cell behaviors such as spreading, proliferation, migration and differentiation.[8–11] Spatial patterning of these signals, such as in a gradient, can result in a concomitant spatial patterning of cellular response.[8, 9, 12] Recently, there have been exciting reports focused on engineering biomaterials that can control cell behaviors through temporal regulation of biomaterial mechanics. For example, the stiffness of cell-laden hydrogels could be decreased or increased through matrix degradation or secondary crosslinking, respectively, of the hydrogel networks.[13–15] However, changes in matrix mechanics are irreversible in these studies, and hence the aforementioned strategies have limitations for understanding the influence of dynamic material mechanics on cellular mechanosensing. Since the extracellular matrix (ECM) is highly dynamic during tissue development or regeneration, [16–18] biomaterial systems with reversibly tunable matrix stiffness are highly desirable in tissue engineering and regenerative medicine.

To address this need, several innovative strategies have been developed to reversibly control hydrogel stiffness. Shih et al. reported using an adamantane-functionalized multi-arm PEG and a β-cyclodextrin (βCD)-modified poly(vinyl alcohol) to form a reversibly tunable hydrogel system based on reversible guest-host interactions between adamantane and βCD.[19] Hörner et al. developed phytochrome-based PEG hydrogels with reversibly tunable mechanical property.[20] However, these systems exhibited limited tunability in

stiffness (from approximately 2.6 to 4.4 kPa). Accardo et al. also reported a photoswitching PEG hydrogel by tethering azobenezene and boronic acid to reversibly regulate the stiffness of hydrogels. However, the range of controllable stiffness was lower than 100 Pa.[21] Rammensee et al. enabled dynamic and reversible modulation of stiffness of polyacrylamide gels based on DNA-mediated crosslinking. However, polyacrylamide gels are often considered toxic and non-biodegradable [22] and their stiffness tunability was still narrow (0.3–3 kPa).[23] Rosales et al. developed a hyaluronic acid hydrogel system with reversible mechanics by sequential photo-degradation and photocrosslinking to soften and then stiffen their hydrogel to apply dynamic mechanical signaling for human mesenchymal stem cells (hMSCs) over a wider range of moduli (from approximately 3 to 30 kPa).[24] However, cells (i.e., hMSCs) were not encapsulated within the hydrogels, but rather on their two-dimensional (2D) surface, which may not be an accurate representation of a physiological cellular microenvironment as it lacks the 3D signals found in native tissues. In addition, the number of softening-stiffening cycles and stiffness range was limited. Liu et al. introduced cyclic stiffness modulation using protein/PEG hydrogels. They could reversibly and dynamically control the stiffness of their hydrogels without limitation of stiffening-softening cycles. However, the storage modulus ratio between stiff and soft hydrogels (G'/G'_0) was approximately 0.85–1, which indicated a very narrow range of stiffness tunability.[25] To the best of our knowledge, there has not been a previous report of a system capable of *in situ* reversible and repeated control of hydrogel mechanics with wide range of stiffness tunability that could be used as an ECM for 3D cell culture.

2. Materials and methods

2.1 Synthesis of OMA

The dual-crosslinkable, biodegradable OMA was prepared by the oxidation and methacrylation of alginates.[26, 27] Briefly, sodium alginate (10 g, Protanal LF 200S, FMC Biopolymer) was dissolved in ultrapure deionized water (diH_2O, 900 ml) overnight. Sodium periodate (0.1 g, Sigma) was dissolved in 100 ml diH_2O, added to the alginate solution under stirring in the dark at room temperature (RT) and then allowed to react for 24 hrs. To synthesize OMA, 2-morpholinoethanesulfonic acid (MES, 19.52 g, Sigma) and NaCl (17.53 g) were directly added to an oxidized alginate (OA) solution (1 L), and the pH was adjusted to 6.5 with 5 N NaOH. N-hydroxysuccinimide (NHS, 2.12 g; Sigma) and 1-ethyl-3-(3-dimethylaminopropyl)-carbodiimide hydrochloride (EDC, 7.00 g; Sigma) (molar ratio of NHS:EDC = 1:2) were added to the mixture to activate 20% of the carboxylic acid groups of the alginate. After 5 min, 2-aminoethyl metharylate (AEMA, 3.04 g) (molar ratio of NHS:EDC:AEMA = 1:2:1) was added to the product, and the reaction was maintained in the dark at RT for 24 hrs. The reaction mixture was precipitated with the addition of acetone in excess, dried in a fume hood, and rehydrated to a 1 w/v % solution in diH_2O for further purification. The OMA was purified by dialysis against diH_2O (MWCO 12000 ~14000, Spectrum Laboratories Inc.) for 3 days, treated with activated charcoal (5 g/L, 50–200 mesh, Thermo Fisher Scientific) for 30 min, filtered (0.22 μm filter) and lyophilized. To determine the levels of alginate oxidation and methacrylation, the OMAs were dissolved in deuterium oxide (D_2O, Sigma) at 2 w/v%, and ^{1}H-NMR spectra were recorded on a Varian Unity-300

(300MHz) NMR spectrometer (Varian Inc.) using 3-(trimethylsilyl)propionic acid-d_4 sodium salt (0.05 w/v%) as an internal standard.

2.2 Fabrication of OMA hydrogels and *in situ* dynamic stiffness tuning

OMA (1.5 w/v%) and CGGGRGDSP (10 mg/g OMA) were dissolved in Dulbecco's Modified Eagle Medium (DMEM, Sigma, St. Louis, MO) overnight with 0.05 w/v % photoinitiator [2-hydroxy-4'-(2-hydroxyethoxy)-2-methylpropiophenone, Sigma] at pH 7.4, placed between quartz (top) and glass (bottom) plates separated by 0.4 mm spacers, and then photocrosslinked with ultraviolet (UV) light (320–500 nm, EXFO OmniCure S1000–1B, Lumen Dynamics Group) at ~20 mW/cm^2 for 1 min to form a photocrosslinked hydrogel (Soft). Photocrosslinked hydrogel disks were created using an 8-mm diameter biopsy punch.

Photocrosslinked hydrogels were stiffened by incubating in 50 mM $CaCl_2$ for 10 min with gentle agitation (Stiff), and then washed three times with Dulbecco's phosphate buffered saline (DPBS). To reversibly soften the hydrogels by removing calcium ions, Stiff hydrogels were incubated in Tris-EDTA (TE, 50 mM Tris, 5 mM EDTA, and pH 7.5) buffer for 10 min with gentle agitation, and then washed three times with DPBS.

2.3 Swelling and degradation of hydrogels

The Soft and Stiff hydrogels were prepared as described above and lyophilized. After dry weights were measured (W_i), dried samples were immersed in 10 ml DMEM and incubated at 37 °C. At predetermined time points, hydrogels were dynamically stiffened or softened by incubating in 50 mM $CaCl_2$ for 10 min with gentle agitation or incubating in TE (50 mM Tris, 5 mM EDTA, and pH 7.5) buffer for 10 min, respectively, washed three times with DPBS, and then further incubated in 10 ml DMEM at 37 °C. For measurement of swelling and degradation, samples were removed, rinsed with DMEM, and the swollen hydrogel sample weights (W_s) were measured. After weighing the swollen hydrogels, they were lyophilized and weighed (W_d). The swelling ratio (Q) was calculated as $Q = W_s/W_d$ (N=4 for each condition per time point). The percent mass loss was calculated as $(W_i - W_d)/W_i \times 100$ (N=4 for each condition per time point).

2.4 Mechanical testing

The elastic moduli of hydrogels were determined by performing uniaxial, unconfined constant strain rate compression testing at RT using a constant crosshead speed of 1%/sec on a mechanical testing machine (225lbs Actuator, TestResources) equipped with a 5 N load cell. Elastic moduli were calculated from the first non-zero linear slope of the stress versus strain plot, and limited to the first 5 % of strain.

2.5 Rheology testing

Dynamic rheological examination of the hydrogel was performed to evaluate with a Kinexus ultra+ rheometer (Malvern Panalytical). In oscillatory mode, a parallel plate (8 mm diameter) geometry measuring system was employed, and the gap was set to 0.36 mm. After the single-crosslinked hydrogel (Soft) was placed between the plates, all the tests were started at 25 °C, and the plate tempearature was maintained at 25 °C. An oscillatory time sweep test at 1 Hz and 1 % shear strain was performed to measure storage moduli (G')

and loss moduli (G") for 1 min. After the measurement, 1 ml $CaCl_2$ solution (50 mM) was carefully applied around the hydrogel disk for 30 min to stiffen the Soft hydrogel, and then an oscillatory time sweep test was performed as described above after removing excess $CaCl_2$ solution. After the measurement, 1 ml Tris-EDTA (TE, 50 mM Tris, 5 mM EDTA, and pH 7.5) buffer solution was carefully applied around the hydrogel disk for 30 min to reversibly soften the hydrogels by removing calcium ions, and then an oscillatory time sweep test was performed as described above after removing excess Tris-EDTA buffer solution. The stiffening and softening were repeated one more time with the oscillatory time sweep tests.

2.6 Encapsulation of hMSCs and human adipose tissue-derived stromal cells (hASCs)

To isolate hMSCs, bone marrow aspirates were obtained from the posterior iliac crest of a healthy twenty three-year old male donor under a protocol approved by the University Hospitals of Cleveland Institutional Review Board.[28, 29] The aspirates were washed with growth medium comprised of low-glucose Dulbecco's Modified Eagle's Medium (DMEM-LG, Sigma) with 10 % prescreened fetal bovine serum (FBS, Gibco). Mononuclear cells were isolated by centrifugation in a Percoll (Sigma) density gradient, and the isolated cells were plated at 1.8×10^5 cells/cm^2 in DMEM-LG containing 10 % FBS, 1 % penicillin/streptomycin (P/S, Thermo Fisher Scientific) in a humidified incubator at 37 °C and 5 % CO_2. After 4 days of incubation, non-adherent cells were removed and adherent cell were maintained in DMEM-LG containing 10 % FBS, 1 % P/S and 10 ng/ml FGF-2 (R&D Systems) with media changes every 3 days. After 14 days of culture, the cells were passaged at a density of 5×10^3 cells/cm^2.

hASCs were isolated from the adipose tissue using a previously reported method.[30] Briefly, lipoaspirates were digested with 200 unit/mg collagenase type I (Worthington Biochemical Products, Lakewood, NJ) for 40 min at 37 °C. The stromal fraction was then isolated by density centrifugation and the stromal cells were plated at 3500 cell/cm^2 on tissue culture plastic in DMEM/nutrient mixture F12 (DMEM/F12, BioWhittaker, Suwance, GA) with 10 % defined fetal bovine serum (FBS, HyClone, Logan, UT) and 1% P/S (BioWhittaker). hASCs at passage 1 were cryopreserved in liquid nitrogen in medium containing 80 % FBS, 10 % DMEM and 10 % dimethyl sulfoxide (Sigma). Upon thawing, hASCs were expanded by plating at 8000 cell/cm^2 in DMEM/F12 containing 10 % FBS (Sigma), 1 % P/S (Thermo Fisher Scientific) and 10 ng/ml FGF-2.

OMA (1.5 w/v %) was dissolved in DMEM with 0.05 w/v % photoinitiator at pH 7.4, and then hMSCs or hASCs (passage number 3, 2×10^6 cells/ml) were suspended in OMA solution. The cell suspended OMA solution was placed between quartz (top) and glass (bottom) plates separated by 0.4 mm spacers and then photocrosslinked with UV light (320–500 nm wavelenth, EXFO Omnicure® S1000–1B, Lumen Dyanmics Group) at ~20 mW/cm^2 for 1 min to form photocrosslinked hydrogel-cell constructs (Soft). Hydrogel/cell-construct disks were created using an 8 mm diameter biopsy punch, placed in wells of 24-well tissue culture plates with 1 ml DMEM-LG (hMSCs) or DMEM/F-12 (hASCs) with 10% FBS, 1% P/S and 10 ng/ml FGF-2 and cultured in a humidified incubator at 37°C with 5% CO_2. Soft hydrogel-cell constructs were stiffened by incubating in 50 mM $CaCl_2$

for 10 min with gentle agitation (Stiff), washed three times with DPBS, and then further cultured the incubator. The Stiff hydrogel-cell constructs were dynamically softened (Soft) by incubating in TE (50 mM Tris, 5 mM EDTA, and pH 7.5) buffer for 10 min to remove calcium ions from stiff hydrogel-constructs, washed three times with DPBS, and then further cultured the incubator. The elastic moduli of the cell encapsulated hydrogel constructs were determined as described above.

2.7 Cell responses in dynamically tunable hydrogels

Cell viability and morphology of encapsulated hMSCs and hASCs in the dynamically tunable hydrogels were investigated using Live/Dead staining comprised of fluorescein diacetate (FDA) and ethidium bromide (EB). The staining solution was freshly prepared by mixing 1 ml FDA solution (1.5 mg/ml in dimethyl sulfoxide, Sigma) and 0.5 ml EB solution (1 mg/ml in PBS, Thermo Fisher Scientific) with 0.3 ml PBS (pH 8). At predetermined time points, 20 μl of staining solution was added into each well and incubated for 3–5 min at room temperature, and then stained hydrogel-cell constructs (3 different samples per group) were imaged (3 different locations per sample) using a fluorescence microscope (ECLIPSE TE 300) equipped with a digital camera (Retiga-SRV).

To quantify the degree of roundness and cell area, image analysis was performed using ImageJ (NIH). To determine cellular domains, Otsu's intensity-based color thresholding method was applied to fluorescence images, and a binary mask was created for each cell. These binary masks were used to calculate cell roundness and spread area. The roundness of cells was calculated as the ratio of the major axis to minor axis length.

To determine the effect of the hydrogel stiffness changes on cell growth, at predetermined time points, some hydrogel-cell constructs were removed from the 24-well plates, put in 1ml cell lysis buffer (Sigma) and homogenized at 35,000 rpm for 30 seconds using a TH homogenizer (Omni International). The homogenized solutions were centrifuged at 500 g with a Sorvall Legent RT Plus Centrifuge (Thermo Fisher Scientific). The supernatants were collected for DNA analysis. DNA content in supernatant was measured using a Picogreen assay kit (Invitrogen) according to the manufacturer's instructions. Fluorescence intensity of the dye-conjugated DNA solution was measured using a fluorescence microplate reader (FMAX, Molecular Devices) set at 485 nm excitation and 538 nm emission.

2.8. Chondrogenesis

To determine the effect of the hydrogel stiffness changes on stem cell fate, hydrogel-hMSC constructs were cultured in chondrogenic differentiation media [1 % ITS+ Premix, 100 nM dexamethasone, 37.5 μg/ml l-ascorbic acid-2-phosphate, 1 mM sodium pyruvate, 100 μM nonessential amino acids, and 10 ng/ml TGF-β1 in HG-DMEM] for 4 weeks. After 2 weeks of culture, the hydrogel constructs were softened or stiffened as described above. After 4 weeks of culture in chondrogenic differentiation media, samples were fixed in 10 % neutral buffered formalin over night at 4 °C, embedded in paraffin, sectioned at a thickness of 10 μm, stained with Toluidine blue O and then imaged using a microscope (Leitz Laborlus S, Leica) equipped with a digital camera (Coopix 995, Nikon). To measure GAG production, chondrogenically differentiated hydrogel constructs were homogenized at 35000 rpm for

60 sec using a TH homogenizer (Omni International) in papain buffer (1 mL, pH 6.5) containing papain (25 μg m/l, Sigma), l-cysteine (2×10^{-3}M, Sigma), sodium phosphate (50×10^{-3}M, Thermo Fisher Scientific) and EDTA (2×10^{-3}M, Thermo Fisher Scientific) and then digested at 65 °C overnight. GAG content was quantified by a dimethylmethylene blue assay [31, 32] and DNA content was measured using the PicoGreen® assay.

2.9. Statistical analysis

All quantitative data are expressed as means± standard deviations. Statistical analyses were performed by one-way analysis of variance (ANOVA) with the Tukey significant difference post hot test using the Origin software (OriginLab). A value of $p<0.05$ was considered statistically significant.

3. Results and discussion

Here, we engineered a cell-laden hydrogel system with reversibly tunable stiffness over a physiologically relevant range using a dual-crosslinkable alginate hydrogel based on photocrosslinking and ionic crosslinking. The overall strategy for the formation of the dynamically tunable alginate hydrogels is depicted in Figure 1. Oxidized methacrylated alginate (OMA) was prepared by functionalizing alginate through both oxidation and methacrylation (Figure S1) to enhance the hydrolytic degradation and to form a dual-crosslinkable alginate hydrogel, respectively. The primary single-crosslinked hydrogel network (Soft) was formed by photopolymerization of the methacrylate groups of OMAs. To generate a dual-crosslinked hydrogel (Stiff), a second crosslinked network was formed by ionic crosslinking of the single-crosslinked alginate hydrogel. The guluronic acid blocks on different alginate chain backbones can form ionic crosslinks with Ca^{2+}, resulting in a dual-crosslinked hydrogel network.

In situ, on-demand hydrogel stiffening was confirmed by measuring the compressive and storage moduli of OMA hydrogels after forming dual-crosslinked networks by incubating in a Ca^{2+}-containing solution. The addition of Ca^{2+} led to stiffening of the single-crosslinked hydrogel (Single_UV; Soft) (Figure 2a). The average compressive (Figure 2b) and storage (Figure S2) moduli range of the hydrogel system spanned approximately 0.5–18 kPa by varying the amount of Ca^{2+}. The compressive modulus of the single-crosslinked OMA hydrogels (Single_UV) was 0.52±0.04 kPa (Figure 2b). As the concentration of Ca^{2+} increased from 3.125 mM (3X) to 50 mM (50X), the compressive moduli of OMA hydrogels were increased from 5.11±0.25 kPa to 18.37±2.13 kPa (Figure 2b), indicating an ability to manipulate hydrogel stiffness by changing the concentration of Ca^{2+}. To demonstrate the dynamic and reversible mechanical property changes of hydrogels, the single-crosslinked (Soft) hydrogel was first incubated in a 50 mM Ca^{2+} solution. The modulus of the hydrogel was increased from 0.57±0.25 kPa (blue bar) to 26.52±9.47 (red bar) kPa within 10 min (Figure 2c). When the stiffened hydrogel was incubated in Tris-ethylenediamine tetraacetic acid (TE) buffer solution for 10 min to remove Ca^{2+}, the modulus of hydrogel was decreased to 1.29±0.19 kPa (green bar). The modulus of this softened hydrogel was further increased to 19.71±5.01 kPa by incubating again in a 50 mM Ca^{2+} solution for 10 min (purple bar). Subsequent hydrogel softening was again achieved

by removing Ca^{2+} ions from the stiffened hydrogel by incubating in TE buffer solution for 10 min (1.21±0.58 kPa, orange bar). To further confirm repeatedly reversible changes in hydrogel mechanics, we performed three stiffening-softening cycles with a different batch of hydrogels. As would be expected, there was no significant difference between the second (purple and orange bars) and third (black and brown bars) states. This trend in the dynamic and reversible stiffness changes was further verified with rheological analysis (Figure 2d). These results demonstrate a unique strategy for on-demand, dynamic and reversible control of hydrogel mechanics by capitalizing on the capacity to bidirectionally convert alginate between single and dual-crosslinking mechanisms.

While numerous studies have investigated the cellular response to static material stiffness on 2D and in 3D matrices, there are only few reports on the effect of dynamic mechanical cues on encapsulated cells in biomaterials [33, 34]. In these studies, however, the number of dynamic stiffness change cycles were limited and the range of the elastic modulus changes was narrow. Thus, to demonstrate that this hydrogel system can be used to repeatedly reversibly change substrate mechanical signals presented to 3D encapsulated cells with a wide range of stiffness, hMSCs were photoencapsulated in single-crosslinked (soft; SO) or dual-crosslinked (stiff; ST) OMA hydrogels, and then the stiffnesses of the hydrogel constructs were decreased or increased every week by removing or adding Ca^{2+}, respectively.

Hydrogels for which crosslinking was not actively changed after initial crosslinking maintained a relatively constant level of swelling (Figure 3a). As would be expected, the swelling ratio of the static SO hydrogels (SO-SO-SO-SO), which were only single-crosslinked, was significantly higher over 4 weeks than that of the static ST hydrogels (ST-ST-ST-ST), which were dual-crosslinked, while the swelling ratio of both groups exhibited minimal variation over time (Figure 3a). In contrast, SO-ST-SO-ST and ST-SO-ST-SO hydrogels exhibited dynamic swelling kinetics. When the hydrogels were additionally crosslinked and stiffened by adding Ca^{2+}, the swelling ratio of hydrogels was decreased. This decreased hydrogel swelling ratio could be increased again by removing Ca^{2+} and thus decreasing the extent of crosslinking and softening them. The mass loss of hydrogels over time was determined as a measure of degradation (Figure 3b). Compared to the static ST hydrogels (ST-ST-ST-ST), the static SO hydrogels (SO-SO-SO-SO) exhibited faster degradation, likely due to a constant lower level of crosslinking in the single-crosslinked constructs. Similar to the swelling ratio changes, the degradation rate of hydrogels was decreased when the hydrogels were additionally crosslinked and stiffened by adding Ca^{2+}. This decreased degradation rate could also be increased by decreasing the degree of crosslinking and softening the hydrogels.

Although the moduli of hydrogels in all groups continuously decreased over time as hydrogels degraded, the moduli of hydrogels could be significantly changed every week via modulation of the extent of crosslinking (Figure 3c and Supplementary Figure S3 and S4) during this degradation. The moduli of the static ST hydrogels (ST-ST-ST-ST) were significantly higher than that of the SO hydrogels (SO-SO-SO-SO) over 4 weeks. The moduli of both hydrogel groups gradually decreased as the hydrogels degraded. The compressive moduli of initially ST hydrogels significantly decreased to 0.18±0.16 kPa

when incubated in TE buffer at the 2nd week (ST-SO-ST-SO). When the *in situ* softened constructs were incubated in Ca^{2+} solution at the 3rd week, the hydrogels could be stiffened again (3.60±2.02 kPa). Similar to the initially ST constructs, the moduli of initially SO constructs significantly increased to 3.37±0.75 kPa (SO-ST-SO-ST) by incubating in Ca^{2+} solution at the 2nd week. When the *in situ* stiffened constructs were incubated in TE buffer at the 3rd week, the constructs were softened again (0.12±0.16 kPa). These stiffened or softened hydrogels could be softened or stiffened by removing or adding Ca^{2+}, respectively, demonstrating the process of stiffening/softening was reversible and repeatable.

To investigate the effect of hydrogel stiffness changes on the viability and morphology of encapsulated hMSCs, the stiffness of hydrogel constructs was changed every week and Live/Dead staining was performed (Supplementary Figure S7 and S8). High cell viability was observed throughout all groups for 4 weeks, indicating the encapsulation process, the macromers and their degradation products and the stiffening and softening of the hydrogel constructs were all cytocompatible (Figure 4a). It should be noted that while cell viability was high, superphysiologic calcium (>10 mM) [35] and/or EDTA [36] concentrations have the potential to affect other cell functions. Since the unreacted calcium ions and EDTA were removed by excess washing with PBS, it is anticipated that the effect of free calcium ions and EDTA in the stiffened and softened hydrogel constructs, respectively, on other encapsulated cell processes would be very limited. The fluorescence photomicrographs showed that almost all of the hMSCs encapsulated in the static ST hydrogels displayed a rounded morphology for 4 weeks (ST, ST-ST, ST-ST-ST and ST-ST-ST-ST). In contrast, hMSCs encapsulated in the static SO hydrogels demonstrated cell spreading at the 1st week and continuously spread for 4 weeks (SO, SO-SO, SO-SO-SO and SO-SO-SO-SO). When the SO hydrogel construct was stiffened at the 1st week and cultured for another week (SO-ST), the morphology of hMSCs was rounded. The rounded morphology of hMSCs in the stiffened hydrogels (SO-ST) changed significantly in the 3rd week to a spread morphology in response to softening hydrogels at the 2nd week (SO-ST-SO) (Figure 4a and b). Similar to the morphology changes of the hMSCs in the 2nd week, the spread morphology of the hMSCs in the softened hydrogels rounded again by stiffening the hydrogel constructs (SO-ST-SO-ST). When the Stiff hydrogel constructs were softened at the 1st week and cultured for another week (ST-SO), the hMSCs started spreading, whereas the hMSCs remained rounded in the static ST hydrogel constructs. The spread morphology of the hMSCs in the softened hydrogels (ST-SO) changed to a rounded morphology in the 3rd week by stiffening the hydrogel constructs (ST-SO-ST). This rounded morphology of the hMSCs in the stiffened hydrogel constructs could be also changed back to a spread morphology by softening the hydrogel constructs again (ST-SO-ST-SO). We also confirmed these results by the quantification of the degree of roundness of the hMSCs (Figure 4b). Cell area was also assessed for each stiffness condition as an indication of cell spreading. As the stiffness of the hydrogel constructs was decreased, cell area increased. Upon stiffening the hydrogel constructs, cell area decreased again. These data indicate the mechanics of hydrogels significantly change the morphology of encapsulated cells, and the hMSCs sense the change of mechanics *in situ*. Since the hydrogel swelling and degradation of these hydrogels are also directly affected by the changes in crosslinking density (Figure 3a and b),

these variables may also have contributed to the cell morphology changes observed in this study.

To evaluate the effect of hydrogel stiffness changes on the growth of the encapsulated hMSCs, the DNA content in the hydrogel constructs was measured every week (Supplementary Figure S5 and S6). The hMSCs encapsulated in the static hydrogels continuously grew for 4 weeks as determined by a DNA content assay, while the DNA content of hMSCs encapsulated in the static SO hydrogels (SO-SO-SO-SO) was significantly higher than that of hMSCs in the static ST hydrogels (ST-ST-ST-ST) (Figure 4d). Importantly, the DNA content of hMSCs encapsulated in the Soft hydrogels decreased when the hydrogel constructs were stiffened at the 1st week (SO-ST-SO-ST). When the stiffened hydrogel constructs were softened again by removing Ca^{2+} the 2nd week, the decreased DNA content of the encapsulated hMSCs recovered. Similar to the SO hydrogel constructs, the DNA content of hMSCs encapsulated in the ST hydrogels could be increase by softening the hydrogel constructs at the 1st week (ST-SO-ST-SO). Subsequent hydrogel constructs stiffening decreased this increased DNA content of encapsulated hMSCs. These results demonstrated that the growth of encapsulated hMSCs was reversibly and repeatedly controllable by stiffening or softening the hydrogel constructs. Similar to the hMSCs, the spreading and growth of hASCs were also controllable by regulating the stiffness of hydrogels (Supplementary Figure S9–S12), demonstrating these findings may be more broadly applicable to multiple cell types.

Stem cell differentiation, such as osteogenesis and chondrogenesis, is affected by the mechanical properties of the encapsulating matrix.[37] Since calcium ions can strongly affect the osteogenesis of stem cells,[38] the effect of hydrogel stiffness changes on encapsulated hMSC chondrogenesis has been investigated to minimize the calcium ions' effect. To investigate the effect of hydrogel stiffness changes on stem cell fate, the stiffness of hMSCs encapsulated SO and ST hydrogel constructs was changed after culture in chondrogenic differentiation media for 2 weeks. After changing the stiffness, the constructs were further cultured in chondrogenic differentiation media for 2 weeks. Similar to the constructs cultured in growth media (Figure 4), the DNA content of hMSCs encapsulated in the soft hydrogels (SO-SO) was significantly higher than the stiff hydrogels (ST-ST) (Figure 5a). Chondrogenic differentiation of hMSCs, quantified by glycosaminoglycan (GAG, Figure 5b) and GAG/DNA (Figure 5c) contents, was significantly greater in the SO-SO hydrogels than the ST-ST hydrogels. This result is well corroborated by other reports where soft hydrogels (<2 kPa) promoted chondrogenesis of MSCs while siffer ones showed less favorable chondrogenesis *in vitro*.[39–41] At 4 weeks, DNA contents increased compared to 2 weeks, while the DNA content of hMSCs encapsulated in the static soft hydrogels (SO-SO-SO-SO) was significantly higher than that of hMSCs in the static stiff hydrogels (ST-ST-ST-ST) during chondrogenesis (Figure 5d). Importantly, the DNA content of hMSCs encapsulated in the SO-SO hydrogels decreased when the constructs were stiffened at the 2nd week (SO-SO-ST-ST). In contrast, the DNA content of hMSCs encapsulated in the ST-ST hydrogels could be increase by softening the constructs at the 2nd week (ST-ST-SO-SO). Similar to construct cellularity, the GAG content of the static soft hydrogel constructs (SO-SO-SO-SO) was significantly higher than that of the static stiff hydrogel constructs (ST-ST-ST-ST) (Figure 5e). Interestingly, the GAG content of the

stiffened soft hydrogel constructs (SO-SO-ST-ST) was significantly higher than that of the static soft hydrogel constructs (SO-SO-SO-SO). Likewise, the GAG content of the softened stiff hydrogel constructs (ST-ST-SO-SO) was significantly higher than that of the static stiff hydrogel constructs (ST-ST-ST-ST). A similar trend was observed even after normalization with DNA (Figure 5f) and further confirmed by Toluidine blue O staining (Figure 5g). As the hydrogel degraded, the compressive modulus of the soft hydrogel construct (SO-SO-SO-SO) was lower than 0.5 kPa at 3 weeks, Figures 3C and S3). Recently, it was shown that chondrogenic differentiation of encapsulated hMSCs was decreased in hydrogels with stiffness was lower than 0.5 kPa compared to hydrogels with stiffness between 0.5 and 2 kPa.[42] Therefore, maintaining the stiffness of hydrogel constructs between 0.5 and 2 kPa, which appears to be a favorable stiffness range for chondrogenesis of MSCs, may be an important design criterion for cartilage tissue engineeering. The stiffened soft hydrogel construct (SO-SO-ST-ST) exhibited the highest GAG production, likely due to maintaining the optimal stiffness for chondrogenesis by *in situ* stiffening after 2 weeks. Previously, the effects of dynamic mechanics on cells have been investigated using alginate-based hydrogels with reversible calcium-crosslinking.[43, 44] In these studies, however, either the cells were not encapsulated within the hydrogels, but rather on their 2D surface for osteogenesis,[43] or only morphological changes, such as cell spreading and migration, were investigated using encapsulated fibroblasts.[44] As mentioned earlier, investigating the osteogenic differentiation of stem cells in matrices stiffened by addition of calcium ions would not be appropriate to investigate the effects of dynamic change of matrix mechanics.

4. Conclusion

This study has demonstrated a potential strategy for on-demand, repeatedly reversible dynamic control of hydrogel mechanics with OMAs via a dual-crosslinking mechanism. The moduli limits of the hydrogels are tunable via varying the second crosslinking density by changing, for example, the concentration of calcium ions in the crosslinking solution or the alginate M/G ratio, molecular weight, or degree of oxidation or methacrylation. By demonstrating direct changes in encapsulated hMSC morphology, cell growth and chondrogenesis in response to dynamic changes in hydrogel mechanics, a repeatedly reversible 3D cellular mechanosensing system has been established. This system provides a powerful tool with a wide range of stiffness tunability to investigate the role of dynamic changes in 3D substrate mechanics in mechanobiology, biological processes and tissue development.

Supplementary Material

Refer to Web version on PubMed Central for supplementary material.

Acknowledgements

The authors would like to thank Dr. Jeffrey Gimble for providing the hASCs. The authors gratefully acknowledge funding from the National Institutes of Health's National Institute of Arthritis and Musculoskeletal and Skin Diseases under award numbers R01AR069564 (EA) and R01AR066193 (EA). The contents of this publication are solely the responsibility of the authors and do not necessarily represent the official views of the National Institutes of Health.

Data availability

The datasets generated and/or analyzed during the current study are available from the corresponding author upon request.

References

[1]. Lutolf MP, Hubbell JA, Synthetic biomaterials as instructive extracellular microenvironments for morphogenesis in tissue engineering, Nature Biotechnology 23(1) (2005) 47–55.

[2]. Jeon O, Alt DS, Linderman SW, Alsberg E, Biochemical and Physical Signal Gradients in Hydrogels to Control Stem Cell Behavior, Advanced Materials 25(44) (2013) 6366–6372. [PubMed: 23983019]

[3]. De Rosa E, Urciuolo F, Borselli C, Gerbasio D, Imparato G, Netti PA, Time and space evolution of transport properties in agarose-chondrocyte constructs, Tissue Engineering 12(8) (2006) 2193–2201. [PubMed: 16968160]

[4]. Barthes J, Ozcelik H, Hindie M, Ndreu-Halili A, Hasan A, Vrana NE, Cell microenvironment engineering and monitoring for tissue engineering and regenerative medicine: the recent advances, Biomed Res Int 2014 (2014) 921905. [PubMed: 25143954]

[5]. Samorezov JE, Alsberg E, Spatial regulation of controlled bioactive factor delivery for bone tissue engineering, Adv Drug Deliv Rev 84 (2015) 45–67. [PubMed: 25445719]

[6]. Jeon O, Lee K, Alsberg E, Spatial Micropatterning of Growth Factors in 3D Hydrogels for Location-Specific Regulation of Cellular Behaviors, Small 14(25) (2018) e1800579. [PubMed: 29782703]

[7]. Dicker KT, Song J, Moore AC, Zhang H, Li Y, Burris DL, Jia X, Fox JM, Core-shell patterning of synthetic hydrogels via interfacial bioorthogonal chemistry for spatial control of stem cell behavior, Chem Sci 9(24) (2018) 5394–5404. [PubMed: 30009011]

[8]. Guilak F, Cohen DM, Estes BT, Gimble JM, Liedtke W, Chen CS, Control of Stem Cell Fate by Physical Interactions with the Extracellular Matrix, Cell Stem Cell 5(1) (2009) 17–26. [PubMed: 19570510]

[9]. Hadden WJ, Young JL, Holle AW, McFetridge ML, Kim DY, Wijesinghe P, Taylor-Weiner H, Wen JH, Lee AR, Bieback K, Vo BN, Sampson DD, Kennedy BF, Spatz JP, Engler AJ, Choi YS, Stem cell migration and mechanotransduction on linear stiffness gradient hydrogels, Proceedings of the National Academy of Sciences of the United States of America 114(22) (2017) 5647–5652. [PubMed: 28507138]

[10]. Zheng Y, Liong Han MK, Jiang Q, Li B, Feng J, del Campo A, 4D hydrogel for dynamic cell culture with orthogonal, wavelength-dependent mechanical and biochemical cues, Materials Horizons 7(1) (2020) 111–116.

[11]. Stowers RS, Allen SC, Suggs LJ, Dynamic phototuning of 3D hydrogel stiffness, Proc Natl Acad Sci U S A 112(7) (2015) 1953–8. [PubMed: 25646417]

[12]. Jeon O, Alsberg E, Regulation of Stem Cell Fate in a Three-Dimensional Micropatterned Dual-Crosslinked Hydrogel System, Adv Funct Mater 23(38) (2013) 4765–4775. [PubMed: 24578678]

[13]. Kloxin AM, Tibbitt MW, Kasko AM, Fairbairn JA, Anseth KS, Tunable Hydrogels for External Manipulation of Cellular Microenvironments through Controlled Photodegradation, Advanced Materials 22(1) (2010) 61-+. [PubMed: 20217698]

[14]. Tamura M, Yanagawa F, Sugiura S, Takagi T, Sumaru K, Kanamori T, Click-crosslinkable and photodegradable gelatin hydrogels for cytocompatible optical cell manipulation in natural environment, Scientific Reports 5 (2015).

[15]. Somo SI, Langert K, Yang CY, Vaicik MK, Ibarra V, Appel AA, Akar B, Cheng MH, Brey EM, Synthesis and evaluation of dual crosslinked alginate microbeads, Acta Biomater 65 (2018) 53–65. [PubMed: 29101016]

[16]. Geckil H, Xu F, Zhang X, Moon S, Demirci U, Engineering hydrogels as extracellular matrix mimics, Nanomedicine (Lond) 5(3) (2010) 469–84. [PubMed: 20394538]

[17]. Daley WP, Peters SB, Larsen M, Extracellular matrix dynamics in development and regenerative medicine, J Cell Sci 121(Pt 3) (2008) 255–64. [PubMed: 18216330]

[18]. Lu P, Takai K, Weaver VM, Werb Z, Extracellular matrix degradation and remodeling in development and disease, Cold Spring Harb Perspect Biol 3(12) (2011).

[19]. Shih H, Lin CC, Tuning stiffness of cell-laden hydrogel via host-guest interactions, Journal of Materials Chemistry B 4(29) (2016) 4969–4974. [PubMed: 32264023]

[20]. Horner M, Raute K, Hummel B, Madl J, Creusen G, Thomas OS, Christen EH, Hotz N, Gubeli RJ, Engesser R, Rebmann B, Lauer J, Rolauffs B, Timmer J, Schamel WWA, Pruszak J, Romer W, Zurbriggen MD, Friedrich C, Walther A, Minguet S, Sawarkar R, Weber W, Phytochrome-Based Extracellular Matrix with Reversibly Tunable Mechanical Properties, Adv Mater 31(12) (2019) e1806727. [PubMed: 30687975]

[21]. Accardo JV, McClure ER, Mosquera MA, Kalow JA, Using Visible Light to Tune Boronic Acid-Ester Equilibria, Journal of the American Chemical Society 142(47) (2020) 19969–19979. [PubMed: 33180484]

[22]. Sanzari I, Humphrey EJ, Dinelli F, Terracciano CM, Prodromakis T, Effect of patterned polyacrylamide hydrogel on morphology and orientation of cultured NRVMs, Sci Rep 8(1) (2018) 11991. [PubMed: 30097609]

[23]. Rammensee S, Kang MS, Georgiou K, Kumar S, Schaffer DV, Dynamics of Mechanosensitive Neural Stem Cell Differentiation, Stem Cells 35(2) (2017) 497–506. [PubMed: 27573749]

[24]. Rosales AM, Vega SL, DelRio FW, Burdick JA, Anseth KS, Hydrogels with Reversible Mechanics to Probe Dynamic Cell Microenvironments, Angewandte Chemie-International Edition 56(40) (2017) 12132–12136. [PubMed: 28799225]

[25]. Liu LM, Shadish JA, Arakawa CK, Shi K, Davis J, DeForest CA, Cyclic Stiffness Modulation of Cell-Laden Protein-Polymer Hydrogels in Response to User-Specified Stimuli Including Light, Advanced Biosystems 2(12) (2018).

[26]. Jeon O, Wolfson DW, Alsberg E, In-Situ Formation of Growth-Factor-Loaded Coacervate Microparticle-Embedded Hydrogels for Directing Encapsulated Stem Cell Fate, Advanced Materials 27(13) (2015) 2216–2223. [PubMed: 25708428]

[27]. Jeon O, Alt DS, Ahmed SM, Alsberg E, The effect of oxidation on the degradation of photocrosslinkable alginate hydrogels, Biomaterials 33(13) (2012) 3503–3514. [PubMed: 22336294]

[28]. Haynesworth SE, Goshima J, Goldberg VM, Caplan AI, Characterization of cells with osteogenic potential from human marrow, Bone 13(1) (1992) 81–8. [PubMed: 1581112]

[29]. Lennon DP, Haynesworth SE, Bruder SP, Jaiswal N, Caplan AI, Human and animal mesenchymal progenitor cells from bone marrow: Identification of serum for optimal selection and proliferation, In Vitro Cellular & Developmental Biology-Animal 32(10) (1996) 602–611.

[30]. Estes BT, Diekman BO, Gimble JM, Guilak F, Isolation of adipose-derived stem cells and their induction to a chondrogenic phenotype, Nature Protocols 5(7) (2010) 1294–1311. [PubMed: 20595958]

[31]. Jeon O, Bin Lee Y, Hinton TJ, Feinberg AW, Alsberg E, Cryopreserved cell-laden alginate microgel bioink for 3D bioprinting of living tissues, Mater Today Chem 12 (2019) 61–70. [PubMed: 30778400]

[32]. Jeon O, Lee YB, Jeong H, Lee SJ, Wells D, Alsberg E, Individual cell-only bioink and photocurable supporting medium for 3D printing and generation of engineered tissues with complex geometries, Materials Horizon 6(8) (2019) 1625–1631.

[33]. Kloxin AM, Kasko AM, Salinas CN, Anseth KS, Photodegradable Hydrogels for Dynamic Tuning of Physical and Chemical Properties, Science 324(5923) (2009) 59–63. [PubMed: 19342581]

[34]. Gillette BM, Jensen JA, Wang MX, Tchao J, Sia SK, Dynamic Hydrogels: Switching of 3D Microenvironments Using Two-Component Naturally Derived Extracellular Matrices, Advanced Materials 22(6) (2010) 686–691. [PubMed: 20217770]

[35]. Wan LQ, Jiang J, Arnold DE, Guo XE, Lu HH, Mow VC, Calcium Concentration Effects on the Mechanical and Biochemical Properties of Chondrocyte-Alginate Constructs, Cell Mol Bioeng 1(1) (2008) 93–102. [PubMed: 19890444]

[36]. Amaral KF, Rogero MM, Fock RA, Borelli P, Gavini G, Cytotoxicity analysis of EDTA and citric acid applied on murine resident macrophages culture, Int Endod J 40(5) (2007) 338–43. [PubMed: 17403041]

[37]. Zigon-Branc S, Markovic M, Van Hoorick J, Van Vlierberghe S, Dubruel P, Zerobin E, Baudis S, Ovsianikov A, Impact of Hydrogel Stiffness on Differentiation of Human Adipose-Derived Stem Cell Microspheroids, Tissue Engineering Part A 25(19–20) (2019) 1369–1380. [PubMed: 30632465]

[38]. Nakamura S, Matsumoto T, Sasaki J, Egusa H, Lee KY, Nakano T, Sohmura T, Nakahira A, Effect of calcium ion concentrations on osteogenic differentiation and hematopoietic stem cell niche-related protein expression in osteoblasts, Tissue Eng Part A 16(8) (2010) 2467–73. [PubMed: 20214455]

[39]. Arora A, Kothari A, Katti DS, Pericellular plasma clot negates the influence of scaffold stiffness on chondrogenic differentiation, Acta Biomaterialia 46 (2016) 68–78. [PubMed: 27693666]

[40]. Kwon HJ, Yasuda K, Chondrogenesis on sulfonate-coated hydrogels is regulated by their mechanical properties (vol 17, pg 337, 2013), Journal of the Mechanical Behavior of Biomedical Materials 28 (2013) 510–510.

[41]. Naqvi SM, McNamara LM, Stem Cell Mechanobiology and the Role of Biomaterials in Governing Mechanotransduction and Matrix Production for Tissue Regeneration, Frontiers in Bioengineering and Biotechnology 8 (2020).

[42]. Moulisova V, Poveda-Reyes S, Sanmartin-Masia E, Quintanilla-Sierra L, Salmeron-Sanchez M, Ferrer GG, Hybrid Protein-Glycosaminoglycan Hydrogels Promote Chondrogenic Stem Cell Differentiation, Acs Omega 2(11) (2017) 7609–7620. [PubMed: 29214232]

[43]. Wei D, Liu AM, Sun J, Chen SP, Wu CH, Zhu H, Chen YJ, Luo HR, Fan HS, Mechanics-Controlled Dynamic Cell Niches Guided Osteogenic Differentiation of Stem Cells via Preserved Cellular Mechanical Memory, Acs Applied Materials & Interfaces 12(1) (2020) 260–274. [PubMed: 31800206]

[44]. Gillette BM, Jensen JA, Wang MX, Tchao J, Sia SK, Dynamic Hydrogels: Switching of 3D Microenvironments Using Two-Component Naturally Derived Extracellular Matrices, Advanced Materials 22(6) (2010) 686-+. [PubMed: 20217770]

Statement of significance:

Since the mechanical properties of native extracellular matrix (ECM) change over time during development, healing and homeostatic processes, it may be valuable to have the capacity to dynamically control the mechanics of biomaterials used in tissue engineering and regenerative medicine applications to better mimic this behavior. Unlike previously reported biomaterials whose mechanical properties can be changed by the user only a limited number of times, this system provides the capacity to induce unlimited alterations to the mechanical properties of an engineered ECM for 3D cell culture. This study presents a strategy for on-demand dynamic and reversible control of materials' mechanics by single and dual-crosslinking mechanisms using oxidized and methacrylated alginates. By demonstrating direct changes in encapsulated human mesenchymal stem cell morphology, proliferation and chondrogenic differentiation in response to multiple different dynamic changes in hydrogel mechanics, we have established a repeatedly reversible 3D cellular mechanosensing system. This system provides a powerful platform tool with a wide range of stiffness tunability to investigate the role of dynamic mechanics on cellular mechanosensing and behavioral responses.

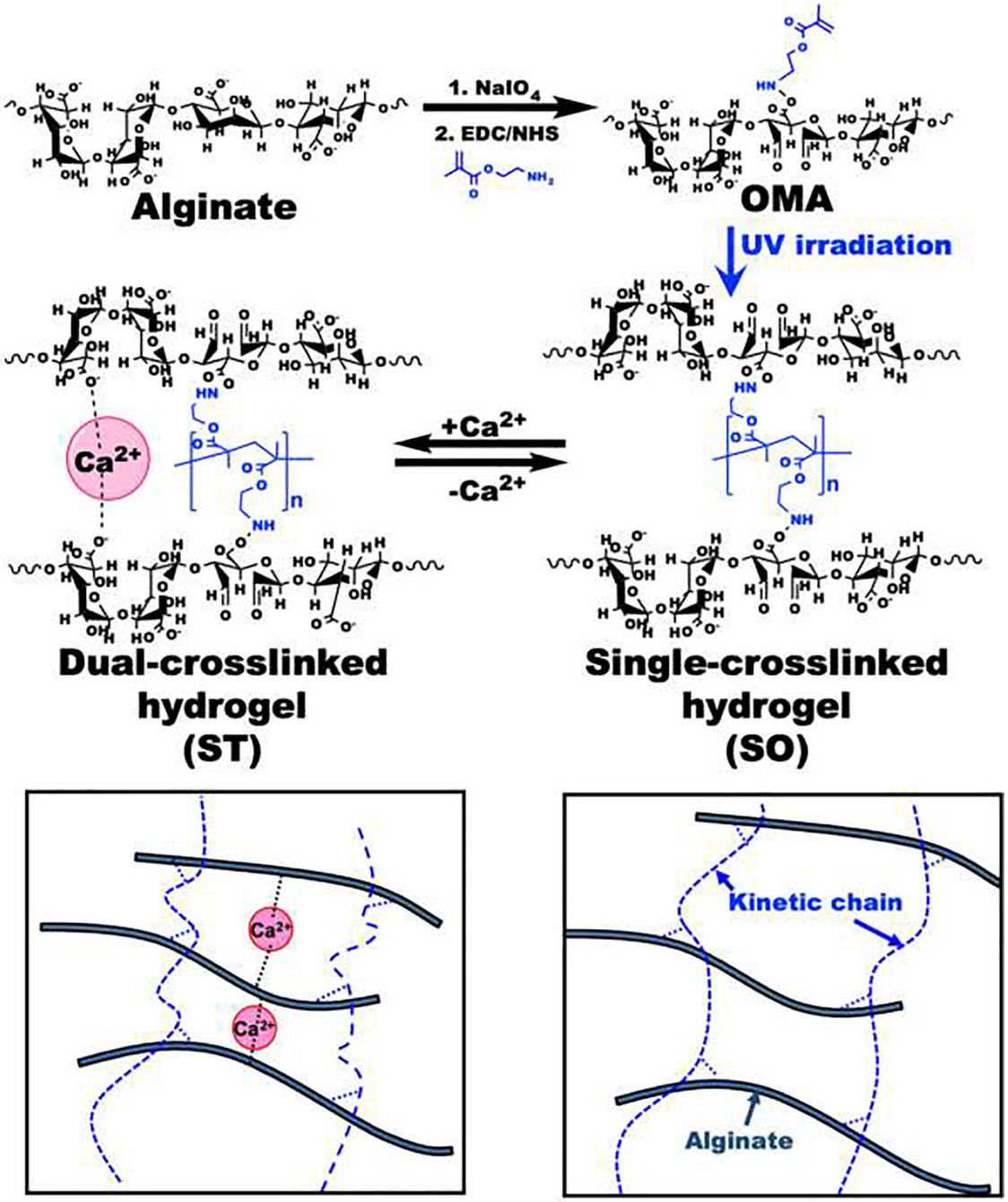

Figure 1.

Schematic illustrations of the preparation and chemical structures of OMA, single-crosslinked soft (SO) and dual-crosslinked stiff (ST) hydrogels.

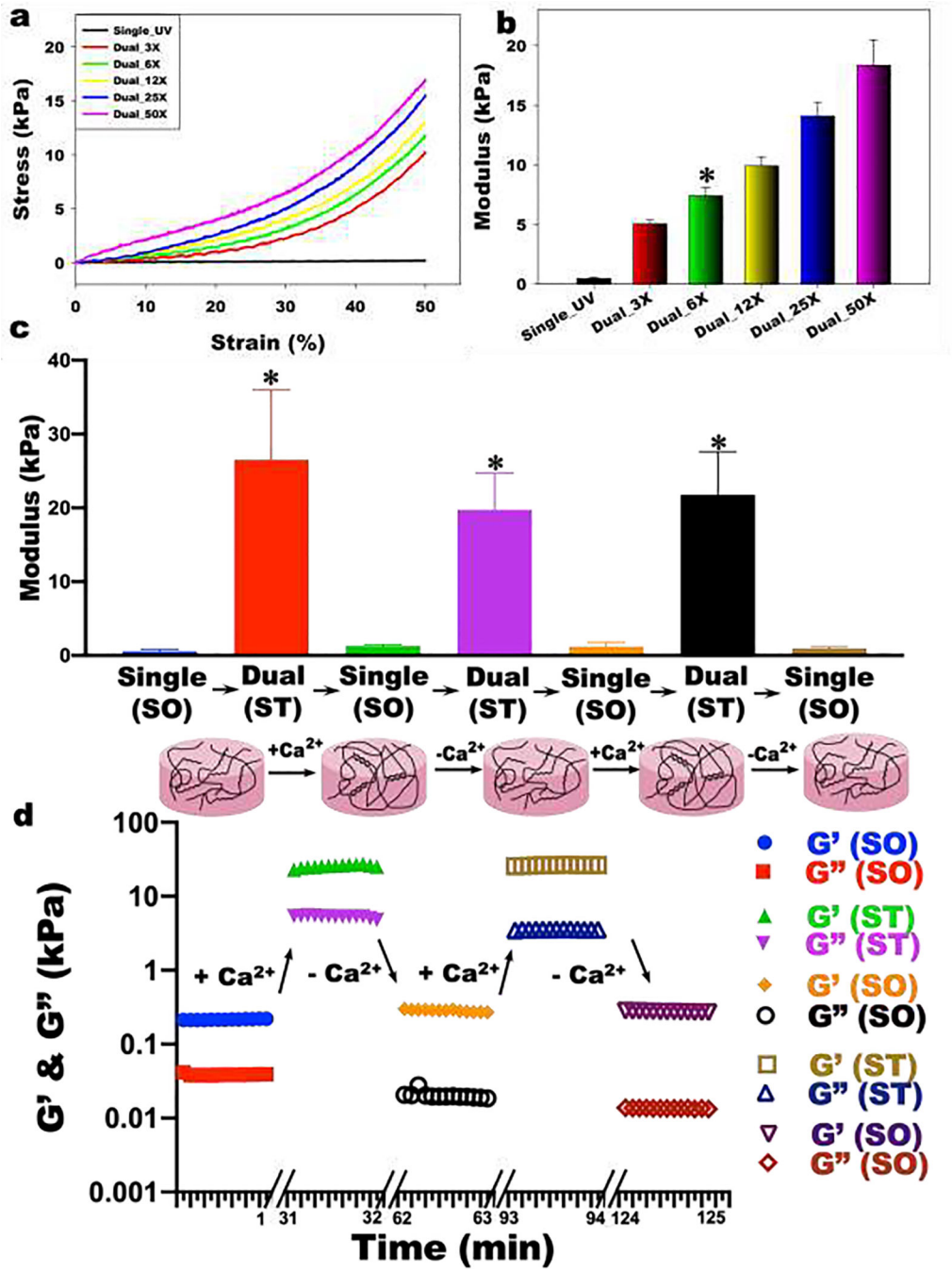

Figure 2.

(a) Representative stress-strain curves and **(b)** compressive modulus of the hydrogels (N=3). The addition of Ca^{2+} led to stiffening of the single-crosslinked SO hydrogel (Single_UV) with various concentration of Ca^{2+} [3.125 mM (3X), 6.25 mM (6X), 12.4 mM (12X), 25 mM (25X) and 50 mM (50X)]. *p>0.05 compared Dual_3X and 12X, otherwise p<0.05. **(c)** Dynamic reversible tuning of hydrogel stiffness. Modulus changes and proposed structures of reversibly tunable hydrogels (N=3). To stiffen the hydrogels, SO hydrogels were incubated in 50X Ca^{2+} solution for 10 min. To soften the hydrogels, ST hydrogels were

incubated in 5X TE buffer (50 mM Tris and 5 mM EDTA at pH 7.5) for 10 min. *$p<0.05$ compared to SO hydrogels. **(d)** Shear moduli changes by stiffening and softening of the hydrogel.

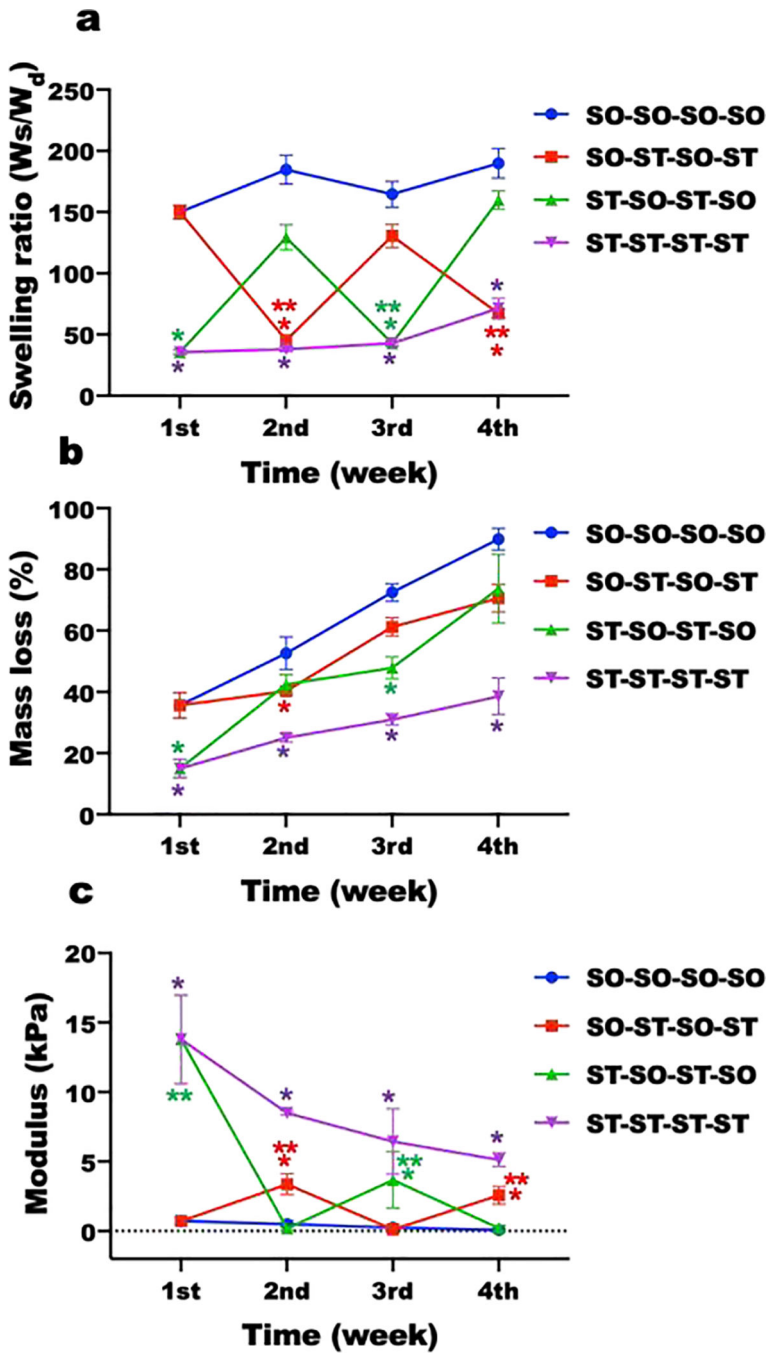

Figure 3.

Physical properties of dynamically tunable hydrogels. **(a)** Swelling ratios (N=4) and **(b)** mass loss (N=4) of hydrogels without cells in DMEM over time. **(c)** Elastic modulus changes of hMSC encapsulated hydrogel constructs in growth media over time (N=4). *p<0.05 compared to soft hydrogels (SO) at a specific time point. **p<0.05 compared to soft hydrogels (SO) within a specific group.

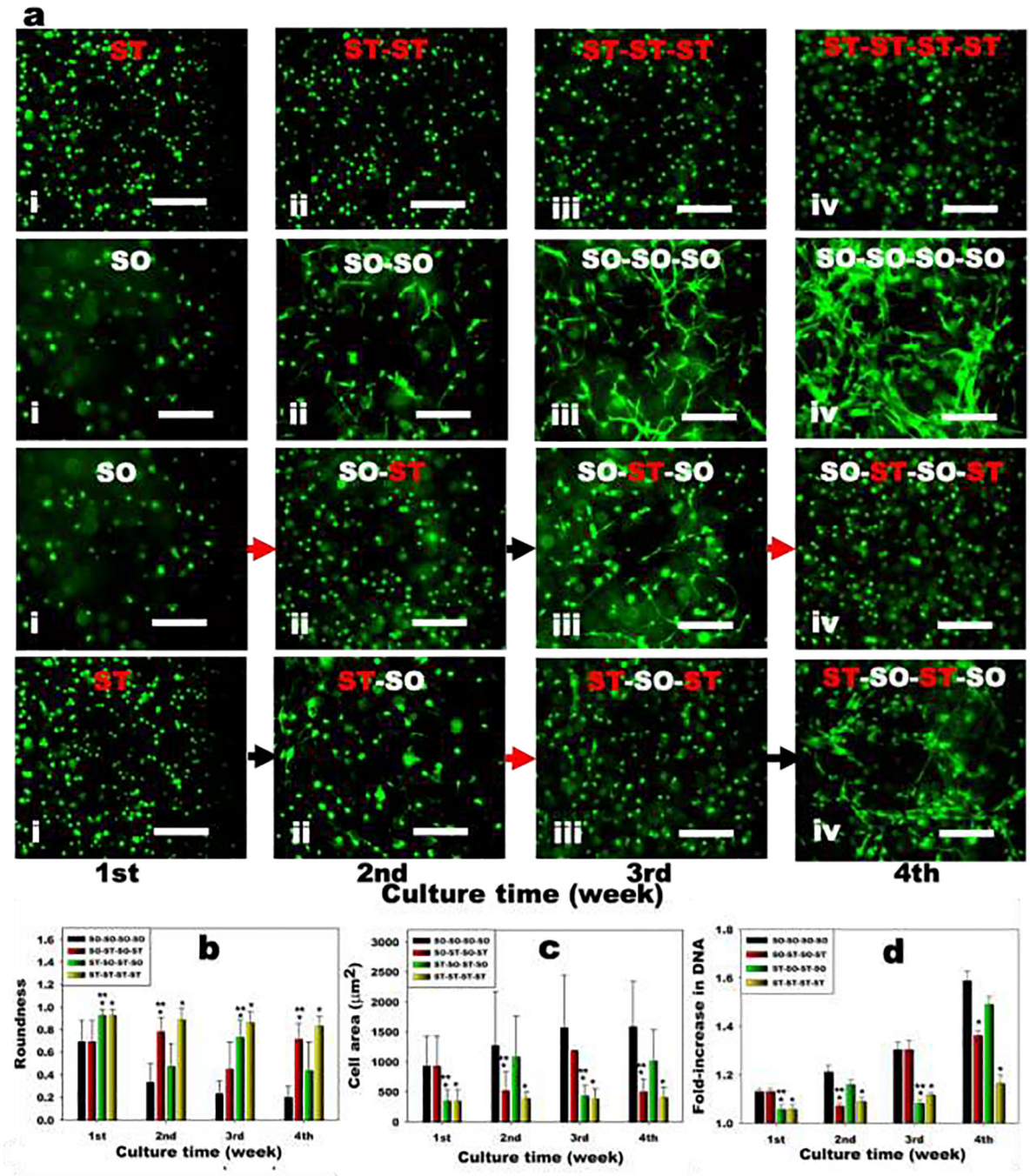

Figure 4.

Encapsulated hMSC response to reversible dynamic hydrogel mechanics in 3D. **(a)** Representative live (green) and dead (red) photomicrographs of encapsulated hMSCs in the hydrogels for 4 weeks. Red arrows indicate stiffening of hydrogels 1 week prior and black arrows mean softening of hydrogels 1 week prior. The scale bars indicate 100 μm. Quantification of cell **(b)** roundness (N=20) and **(c)** area (N=20) within the hydrogels. **(d)** Quantification of DNA content in hMSC encapsulated hydrogels over time (N=4). Black bars = SO-SO-SO-SO, Red bars = SO-ST-SO-ST, Green bars = ST-SO-ST-SO and Yellow

bars = ST-ST-ST-ST. *$p<0.05$ compared to soft hydrogels (SO) at a specific time point. **$p<0.05$ compared to soft hydrogels (SO) within a specific group.

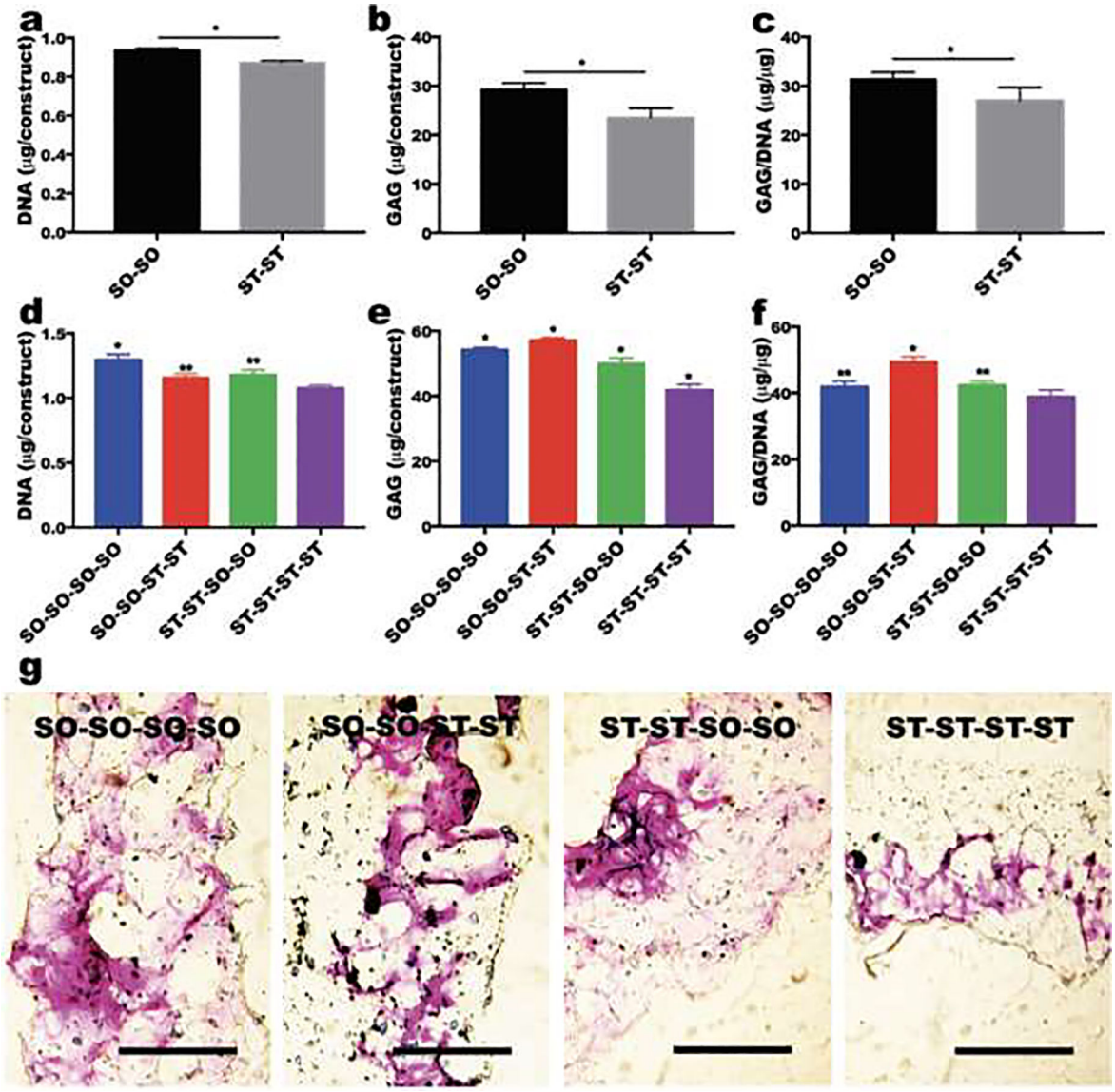

Figure 5.

The effect of stiffness changes on chondrogenesis of encapsulated hMSCs. Quantification of (a) DNA, (b) GAG and (c) GAG/DNA in hMSCs encapsulated within hydrogels after 2 weeks of culture in chondrogenic differentiation media (N=4). *$p<0.05$. Quantification of (d) DNA, (e) GAG and (f) GAG/DNA in hMSCs encapsulated within hydrogels after 4 weeks of culture in chondrogenic differentiation media (N=4). *$p<0.05$ compared to the other groups and **$p<0.05$ compared to ST-ST-ST-ST group. (g) Toluidine blue O staining of sectioned hydrogel constructs after 4 weeks of culture in chondrogenic differentiation media. The scale bars indicate 500 μm.